Effect of Phosphorus Axial π-Acceptors in Iron(III) Porphyrinates: Characterization of Low-Spin Complexes $[(PPh(OMe)_2)_2Fe(T(p\text{-}Me)PP)]CF_3SO_3$ and $[(PPh(OEt)_2)_2Fe(T(p\text{-}Me)PP)]CF_3SO_3$

Marie-Agnès Pilard,[†] Maud Guillemot,[†] Loïc Toupet,[‡] J. Jordanov,[§] and Gérard Simonneaux*,[†]

Laboratoire de Chimie Organométallique et Biologique, URA CNRS 415, Université de Rennes 1, 35042 Rennes Cedex, France, Groupe de Physique Cristalline, UA CNRS 040804, Université de Rennes 1, Campus de Beaulieu, 35042 Rennes Cedex, France, and Service de Chimie Inorganique et Biologique, CENG, 38054 Grenoble Cedex, France

Received April 25, 1997[⊗]

The synthesis and characterization of the trifluoromethanesulfonato derivatives of bis(dimethyl phenylphosphonite)(tetrakis(*p*-methylphenyl)porphyrinato)iron^{III}, **1**, and bis(diethyl phenylphosphonite)(tetrakis(*p*-methylphenyl)porphyrinato)iron^{III}, **2**, are reported: $[(PPh(OMe)_2)_2Fe(T(p\text{-}Me)PP)]CF_3SO_3$, **1**, and $[(PPh(OEt)_2)_2Fe(T(p\text{-}Me)PP)]CF_3SO_3$, **2**, (T(*p*-Me)PP = tetrakis(*p*-methylphenyl)porphyrinato). The crystal structure of complexes **1** and **2** have been determined. Both X-ray structures show that the porphyrinate rings are strongly ruffled. The equatorial Fe−N bond distances average to 1.971 (6) Å for **1** and to 1.969 (7) Å for **2**, which is a quite short distance for low-spin iron^{III} porphyrinate derivatives. The ^{1}H NMR isotropic shifts at 20 °C of the pyrrole protons of the two complexes, varied from −2 ppm for **2** to +3 ppm for **1** rather than the expected −20 to −30 ppm, based on previously studied bis-ligated complexes of low-spin ferric porphyrins. The electron paramagnetic resonance spectra of $[(PPh(OMe)_2)_2Fe(T(p\text{-}Me)PP)]CF_3SO_3$, **1**, and $[(PPh(OEt)_2)_2Fe(T(p\text{-}Me)PP)]CF_3SO_3$, **2**, in solution are axial, with $g_\perp = 2.36$ and $g_\parallel = 1.87-1.91$ at 4 K, $\Sigma g^2 = 14.7$. The Mössbauer spectra of **1** and **2** at 70 K have isomer shifts of 0.35 and 0.37 mm/s and quadrupole splittings of 1.23 and 1.66 mm/s, respectively. All physical properties are consistent with a low-spin iron^{III} with an unusual ground-state configuration $(d_{xz},d_{yz})^4(d_{xy})^1$, as recently reported for $[(4\text{-}CN\text{-}Py)_2Fe(TPP)]ClO_4$ Safo, (M. K.; Walker, F. A.; Raitsimring, A. M.; Walters, W. P.; Dolata, D. P.; Debrunner P. G.; Scheidt, W. R. *J. Am. Chem. Soc.* **1994**, *116*, 7760−7770). Crystal data for $[(PPh(OMe)_2)_2Fe(T(p\text{-}Me)PP)]CF_3SO_3$, **1:** $a = 16.611(3)$ Å, $c = 20.722(4)$ Å, trigonal, space group $P3_2$, $V = 4951(2)$ Å^3, $Z = 3$. Crystal data for $[(PPh(OEt)_2)_2Fe(T(p\text{-}Me)PP)]CF_3SO_3$, **2:** $a = 24.017(2)$ Å, $b = 14.380(9)$ Å, $c = 18.702(4)$ Å, monoclinic, space group $P2_{1/a}$, $V = 6457(6)$ Å^3, $Z = 4$.

Introduction

Although phosphines and other group VB donors are not natural substrates in biological systems, their interactions with hemoglobins,[1] myoglobins,[2] cytochromes P-450,[3] chloroperoxidase,[4] cytochrome *c*,[5] and metalloporphyrins[6,7] have been widely studied. This interest in phosphorus derivatives derives from their strong binding to those metalloproteins which bind or utilize molecular oxygen and their consequent ability to be an important tool in the characterization of hemoproteins. In comparison with the amount of information available for bonds to phosphines, relatively few parameters are known for bonds to phosphonite and phosphite ligands in complexes of metals in positive oxidation states.[8] In this paper, we present results on complexation of phosphonite to ferriporphyrins that enable us to compare phosphines and phosphonites in very closely related complexes.

[†] Laboratoire de Chimie Organométallique et Biologique.
[‡] Groupe de Physique Cristalline.
[§] Service de Chimie Inorganique et Biologique.
[⊗] Abstract published in *Advance ACS Abstracts,* December 1, 1997.

(1) (a) Wilkinson, G. *Nature* **1951**, *168*, 514. (b) Simonneaux, G.; Bondon, A.; Brunel, C.; Sodano, P. *J. Am. Chem. Soc*. **1988**, *110*, 7637. (c) Bondon, A.; Simonneaux, G. *Biophys. Chem*. **1990**, *37*, 407. (d) Brunel, C.; Bondon, A.; Simonneaux, G. *J. Am. Chem. Soc*. **1994,** *116*, 11827.
(2) (a) Bondon, A.; Petrinko, P.; Sodano, P.; Simonneaux, G. *Biochim. Biophys. Acta* **1986**, *872*, 163. (b) Simonneaux, G.; Bondon, A.; Sodano, P. *Inorg. Chem.* **1987**, *26*, 3636. (c) Brunel, C.; Bondon, A.; Simonneaux, G. *Biochim. Biophys. Acta* **1992**, *1101*, 73 . (d) Brunel, C.; Bondon, A.; Simonneaux, G. *Eur. J. Biochem.* **1993**, *214*, 405.
(3) (a)Wiley, R. A.; Sternson, L. A.; Sasame, H. A.; Gillette, J. R. *Biochem. Pharmacol.* **1972**, *21*, 3235. (b) Mansuy, D.; Duppel, W.; Ruf, H. H.; Ullrich, V. *Hoppe-Seyler's Z. Physiol. Chem*. **1974,** *355*, 1341. (c) White, R. E.; Coon, M. J. *J. Biol. Chem.* **1982**, *257*, 3073. (d) Anderssson, L. A.; Sono, M.; Dawson, J. H. *Biochim. Biophys. Acta* **1983**, *748*, 341.
(4) (a) Sono, M.; Dawson, J. H.; Hager, L. P. *Inorg. Chem.* **1985**, *24*, 4339. (b) Sono, M.; Dawson, J. H.; Hall, K.; Hager, L. P *Biochemistry* **1986**, *25*, 347. (c) Sono, M.; Hager, L. P.; Dawson, J. H. *Biochim. Biophys. Acta* **1991**, *1078*, 351.
(5) (a) Schejter, A.; Plotkin, B.; Vig, I. *FEBS Lett.* **1991**, *280*, 199. (b) Legrand, N.; Bondon, A.; Simonneaux, G.; Shejter, A. *Magn. Reson. Chem.* **1993**, *31*, S23. (c) Legrand, N.; Bondon, A.; Simonneaux, G. *Inorg. Chem.* **1996**, *35*, 1627.
(6) For examples of phosphine-ferric porphyrin derivatives, see: (a) Ruf, H. H.; Wende, P. *J. Am. Chem. Soc*. **1977**, *99*, 5499. (b) Ruf, H. H.; Wende, P.; Ullrich, W. J. *Inorg. Biochem.* **1979**, *11*, 189. (c) Sodano, P.; Simonneaux, G. *Inorg. Chem*. **1988**, *27*, 3956. (d) Toupet, L.; Sodano, P.; Simonneaux, G. *Acta Crystallogr*. **1990**, *C46*, 1631.
(7) For examples of phosphine-ferrous porphyrins, see: (a) Spiro, T. J.; Burkle, J. M. *J. Am. Chem. Soc.* **1976**, *98*, 5482. (b) La Mar, G.; Del Gaudio, J. *Bioinorg. Chem.* **1977**, *2*, 207. (c) Ohya, T.; Morohoshi, H.; Sato, M. *Inorg. Chem*. **1984**, *23*, 1303. (d) Stynes, D. V.; Fletcher, D.; Chen, X. *Inorg. Chem*. **1986**, *25*, 3483. (e) Belani, R. M.; James, B. R.; Dolphin, D.; Rettig, S. T. *Can. J. Chem.* 1988, *66*, 2072. (f) Simonneaux, G.; Sodano P. *Inorg Chem.* **1988**, *27*, 3956. (g) Mink, L. M.; Christensen, K. A.; Walker, F. A. *J. Am. Chem. Soc.* **1992**, *114*, 6930. (h) Mink, L. M.; Polam, J. R.; Christensen, K. A.; Bruck, M. A.; Walker, F. A. *J. Am. Chem. Soc.* **1995,** *117*, 9329. (i) Polam, J. R.; Wright, J. L.; Christensen, K. A.; Walker, F. A.; Flint, H.; Grodzicki, M.; Trautwein, A. X. *J. Am. Chem. Soc.* **1996**, *118*, 5272.
(8) Collman, J. P.; Hegedus, L. S. In *Principles ans Applications of Organotransition Metal Chemistry*; Kelly, A., Ed.; University Science Books: Mill Valley, CA, 1980; pp 54−60.

S0020-1669(97)00484-9 CCC: $14.00

There is currently a large interest in determining what factors affect the electronic structure of low-spin hemoproteins. Walker and Simonis[9] have shown that proton NMR spectroscopy is a sensitive tool for probing the unpaired electron density distribution in low-spin iron^{III} porphyrins. It has been accepted that most of the low-spin iron^{III} have a $(d_{xy})^2(d_{xz}, d_{yz})^3$ ground state. Some time ago, La Mar and co-workers[10] first recognized that the hyperfine shifts for both the pyridine ligands and the porphyrin are very sensitive to the basicity of the axial ligands. More recently, we reported that, when two molecules of *tert*-butylisocyanide are bound to ferric tetraphenylporphyrin, the ^{1}H NMR spectrum is indicative of a low-spin complex.[11] The hyperfine shifts were separated into their dipolar and contact contributions. The separated components reflect the very low magnetic anisotropy of the iron, and the unusual orientation of the unpaired spin density when the nitrogen axial ligands are exchanged for isocyanide ligands leads to complete reverse localization.[11,12] Subsequently, it was recognized that the unusual NMR behavior results from the formation of an unusual $(d_{xy})^1$ ground state.[9] It should be underlined that a similar situation was very recently reported with low-basicity cyanopyridine complexation to ferriporphyrins.[13] The change in ground state of low-spin iron^{III} from $(d_{xy})^2(d_{xz},d_{yz})^3$ to $(d_{xz},d_{yz})^4(d_{xy})^1$ electron configuration occurs progressively through the series of pyridine complexes of both Fe^{III}TPP (TPP: tetrakisphenyl porphyrinate) and Fe^{III}TMP (TMP: tetrakismesityl porphyrinate) complexes, the low-basicity pyridines stabilizing the unusual $(d_{xz},d_{yz})^4(d_{xy})^1$ state. The axial electron paramagnetic resonance (EPR) spectra, with $g_\perp > g_{||}$ are also indicative of a $(d_{xz},d_{yz})^4(d_{xy})^1$ state. With the TPP compound, the X-ray structure shows that the two axial ligands have relative perpendicular orientations along with an extensively S_4-ruffled porphyrin core which is related to electronic factors rather than steric factors. This electronic contribution may be due to the partial delocalization of the $(d_{xy})^1$ unpaired electron into the $3a_{2u}$-(π) orbital of the porphyrin ring, which is made possible by the twisting of the nitrogen p_z orbitals of the nitrogen out of the plane of the porphyrin ring, as suggested recently.[9,12,13b] The Mössbauer spectrum shows also an unusually small positive to large negative[13] quadrupole splitting in the ferric tetraphenylporphyrinato complexes.

In an attempt to provide additional pertinent information for determining what factors affect the electronic structure of low-spin hemoproteins, phosphonite complexes of ferric porphyrins were investigated. These complexes are relatively difficult to prepare (see Experimental Section) but allow comparisons of variation in chemical shifts with changing the organic substituents on phosphorus, while the stereochemistry and the spin state remain constant. In addition, useful information can be obtained from comparison with phosphine ligands that are weaker π acceptors than phosphonites.[14−16] We previously observed an unusual electronic structure for [(PPh(OMe)$_2$Fe(TPP)]ClO$_4$ by ^{1}H NMR.[17] We have now further extended our studies to the preparation and complete spectral characterization (NMR, EPR, and Mössbauer) of [(PPh(OMe)$_2$)$_2$Fe(TPP)]CF$_3$SO$_3$ and [(PPh(OEt)$_2$)$_2$Fe(TPP)]CF$_3$SO$_3$. The X-ray structures of [(PPh(OMe)$_2$)$_2$Fe(T(*p*-Me)PP)]CF$_3$SO$_3$ (T(*p*-Me)PP = tetrakis(*p*-methylphenyl)porphyrinato) and [(PPh(OEt)$_2$)$_2$Fe(T(*p*-Me)PP)]CF$_3$SO$_3$ have also been determined. A comparison with [(PPh(Me)$_2$)$_2$Fe(TPP)]ClO$_4$[6c,d] suggests an electronic contribution to the observed ruffling of the porphyrin ring in the bisphosphonite complexes.

Experimental Section

General Information. As a precaution against the formation of the μ-oxo dimer [Fe(TPP)]$_2$O[18] all reactions were carried out in dried solvents in Schlenk tubes under an Ar atmosphere. Solvents were distilled from appropriate drying agents and stored under argon. ^{1}H NMR spectra were recorded on a Bruker AC 300P spectrometer in CD_2Cl_2 or $CDCl_3$ at 300 MHz. Tetramethylsilane was used as internal reference. The temperatures are given within 1 K. EPR spectra were recorded on a Varian E 109 spectrometer operating at ca. 9 GHz and equipped with a gaussmeter and a microwave frequency counter for respective monitoring of the field and of the frequency. Samples were cooled to 4.2 K in a stream of helium gas in frozen CH_2Cl_2, the temperature of which was controlled by an Oxford Instruments ESR 900 cryostat. Mössbauer spectra were recorded at Toulouse in the solid state at 80 and 4 K. Visible spectra were measured on a Uvikon 941 spectrometer in CH_2Cl_2. Elemental analyses were performed by the Service Central of Analyses (CNRS) at Vernaison, France.

Caution: We have not observed detonation of iron porphyrin perchlorates under our conditions, but care is urged.

Reagents. The following iron porphyrins[19] were prepared by literature methods: [Fe (TPP)]ClO$_4$,[20] [Fe(T(*m*-Me)PP)]ClO$_4$,[20,21] [Fe(T(*p*-Me)PP)]ClO$_4$,[21] [Fe(TPP)]CF$_3$SO$_3$,[20] [Fe(T(*m*-Me)PP)]CF$_3$SO$_3$,[21] and [Fe(T(*p*-Me)PP)]CF$_3$SO$_3$.[21] P(OMe)$_2$Ph and P(OEt)$_2$Ph are commercially available.

Synthesis. [(P(OMe)$_2$Ph)$_2$Fe(T(*p*-Me)PP)]CF$_3$SO$_3$, **1**. To a solution of 0.21 g (0.24 mmol) of [Fe(T(*p*-Me)PP)]CF$_3$SO$_3$ in 10 mL of dichloromethane was added 10 equiv of P(OMe)$_2$Ph by a syringe under stirring at room temperature. Then 40 mL of pentane was added and the solution was set aside 2 days for crystallization at 0 °C. Purple crystals of [(P(OMe)$_2$Ph)$_2$Fe(T(*p*-Me)PP)]CF$_3$SO$_3$ were collected by filtration and washed with hexane. Yield: 0.22 g (80%). UV−vis (CH_2Cl_2): λ_{max}/nm 358 (ϵ = 19.6 dm^3 mmol^{-1} cm^{-1}), 437 (ϵ = 37.5), 552 (ϵ = 6.3), 607 (ϵ = 5.8).

[(P(OEt)$_2$Ph)$_2$Fe(T(*p*-Me)PP)]CF$_3$SO$_3$, **2**. To a solution of 0.20 g (0.23 mmol) of [Fe(T(*p*-Me)PP)]CF$_3$SO$_3$ in 16 mL of dichloromethane was added 8 equiv of P(OEt)$_2$Ph by a syringe under stirring at room temperature. Then 60 mL of pentane was added, and the solution was set aside 2 days for crystallization at 0 °C. Purple crystals of [(P(OEt)$_2$Ph)$_2$Fe(T(*p*-Me)PP)]CF$_3$SO$_3$ were collected by filtration and washed with hexane. Yield: 0.20 g (72%). Anal. Calcd for $C_{69}H_{66}N_4P_2O_7F_3SFe$: C, 65.23; H, 5.20; N, 4.41; P, 4.88. Found: C, 65.06; H, 5.00; N, 4.52; P, 4.77. UV−vis (CH_2Cl_2): λ_{max}/nm 356 (ϵ = 24 dm^3 mmol^{-1} cm^{-1}), 438 (ϵ = 50), 556 (ϵ = 5.8), 608 (ϵ = 5.3).

(9) Walker, A.; Simonis, U. In *Biological Magnetic Resonance*; Berliner, L. E., Reuben, J., Eds.; Plenum: New York, 1993; Vol. 12, p 132 and references therein.
(10) (a) La Mar, G. N.; Bold, T. J.; Satterlee, J. D. *Biochim. Biophys. Acta* **1977,** *498*, 189. (b) La Mar, G. N.; Del Gaudio, J.; Frye, J. S. *Biochim. Biophys. Acta* **1977**, *498*, 422.
(11) (a) Simonneaux, G.; Hindré, F.; Le Plouzennec, M. *Inorg. Chem*. **1989**, *28*, 823. (b) Gèze, C.; Legrand, N.; Bondon, A.; Simonneaux, G. *Inorg. Chim. Acta* **1992**, *195*, 73.
(12) Walker, F. A.; Nasri, H.; Turowska-Tyrk, I.; Mohanrao, K.; Watson, C. T.; Shokhirev, N. V.; Debrunner, P. G.; Scheidt, W. R. *J. Am. Chem. Soc.* **1996**, *118*, 12109.
(13) (a) Safo, M. K.; Gupta, G. P.; Watson, C. T.; Simonis, U.; Walker, F. A.; Scheidt, W. R. *J. Am. Chem. Soc*. **1992**, *114*, 7066. (b) Safo, M. K.; Walker, F. A.; Raitsimring, A. M.; Walters, W. P.; Dolata, D. P.; Debrunner, P. G.; Scheidt, W. R. *J. Am. Chem. Soc*. **1994**, *1*, 7760. (c) Cheesman, M. R.; Walker, F. A. *J. Am. Chem. Soc.* **1996**, *118*, 7373.
(14) The presence of oxygen atoms bound to the phosphorus decreases the basicity and increases the π acidity of the ligand. This is the case of phosphites and to a less extent of phosphonites. For examples, see: refs 8, 15−16.
(15) Tolman, C. A. *Chem. Rev*. **1977,** *77*, 313.
(16) Crabtree, R. H. In *The Organometallic Chemistry of the Transition Metals*; Wiley-Interscience: New York, 1988; p 71.
(17) Guillemot, M.; Simonneaux, G. *J. Chem. Soc., Chem. Commun.* **1995**, 2093.
(18) Fleisher, E. B.; Palmer, J. M.; Srivastava, T. S.; Chatterjee, A. *J. Am. Chem. Soc.* **1971**, *93*, 3162.
(19) Abbreviations used: H$_2$(TPP), tetraphenylporphyrin; H$_2$[T(*m*-Me)PP], tetrakis(*m*-methylphenyl)porphyrin; H$_2$[T(*p*-Me)PP], tetrakis(*p*-methylphenyl)porphyrin.
(20) Reed, C. A.; Mashiko, T.; Bentley, S. P.; Kasner, M. E.; Scheidt, W. R.; Spartalian, K.; Lang, G. *J. Am. Chem. Soc*. **1979**, *101*, 2948.
(21) Goff H.; Shimomura, E. *J. Am. Chem. Soc*. **1980**, *102*, 31.

Table 1. Crystallographic Data for $[(P(OMe)_2Ph)_2Fe(T(p\text{-}Me)PP)]CF_3SO_3$, **1**, and $[(P(OEt)_2Ph)_2Fe(T(p\text{-}Me)PP)]CF_3SO_3$, **2**

	1·$2CH_2Cl_2$	**2**
empirical formula	$C_{67}H_{62}Cl_4FeF_3N_4O_7P_2S$	$C_{69}H_{66}FeF_3N_4O_7P_2S$
fw	1383.93	1270.71
crystal system	trigonal	monoclinic
space group	$P3_2$	$P2_1/a$
a, Å	16.611(3)	24.017(2)
b, Å		14.380(9)
c, Å	20.722(4)	18.702(4)
α, deg		
β, deg		91.48(1)
γ, deg		
V, Å^3	4951(2)	6457(6)
Z	3	4
P calcd g cm^{-3}	1.392	1.306
μ cm^{-1}	5.303	3.739
T (K)	293	293
R_w	0.062	0.069
final R	0.066	0.072

For the preparation of the tetraphenyl and *meta*-methylated derivatives, the same procedure can be used with the corresponding perchlorate or triflate analogues in dichloromethane solvent and the suitable ligand. However, for *meta*-methyl derivatives, a partial decomposition was observed; the solutions were reduced in volume to ensure precipitation, due to the high solubility of *meta*-methyl derivatives in dichloromethane.

$[(P(OMe)_2Ph)_2Fe(TPP)]CF_3SO_3$. Yield: 78%. UV−vis ($CH_2Cl_2$): λ_{max}/nm 358 (ϵ = 19.6 dm^3 mmol^{-1} cm^{-1}), 437 (ϵ = 37.5), 554 (ϵ = 6.3), 606 (ϵ = 5.2).

$[(P(OEt)_2Ph)_2Fe(TPP)]CF_3SO_3$. Yield: 82%. Anal. Calcd for $C_{65}H_{58}N_4P_2O_7F_3SFe$: C, 64.30; H, 4.78; N, 4.61; P, 5.11. Found: C, 63.94; H, 5.06; N, 4.68; P, 4.22. UV−vis (CH_2Cl_2): λ_{max}/nm 356 (ϵ = 24 dm^3 mmol^{-1} cm^{-1}), 438 (ϵ = 39), 556 (ϵ = 5.8), 608 (ϵ = 5.3).

$[(P(OMe)_2Ph)_2Fe(TPP)]ClO_4$. To a solution of 0.19 g (0.24 mmol) of $[Fe(TPP)]ClO_4$ in 20 mL of dichloromethane was added 8 equiv of $P(OMe)_2Ph$ by a syringe at room temperature. The solution was set aside overnight for crystallization at 0 °C. Fine crystals of $[(P(OMe)_2Ph)_2Fe(TPP)]ClO_4$ were collected by filtration and washed with hexane. Yield: 0.21 g (74%). Anal. Calcd for $C_{60}H_{50}N_4P_2O_8ClFe$, CH_2Cl_2: C, 61.38; H, 4.36; N, 4.69; P, 5.19. Found: C, 61.64; H, 4.25; N, 5.26; P, 4.79. UV−vis (CH_2Cl_2): λ_{max}/nm 357 (ϵ = 28 dm^3 mmol^{-1} cm^{-1}), 437 (ϵ = 59), 553 (ϵ = 7), 605 (ϵ = 5.3).

$[(P(OMe)_2Ph)_2Fe(T(p\text{-}Me)PP)]ClO_4$. Yield: 85%. Anal. Calcd for $C_{64}H_{58}N_4P_2O_8ClFe$: C, 66.02; H, 5.02; N, 4.81; P, 5.32. Found: C, 65.85; H, 5.18; N, 4.85; P, 5.09. UV−vis (CH_2Cl_2): λ_{max}/nm 358 (ϵ = 26 dm^3 mmol^{-1} cm^{-1}), 437 (ϵ = 60), 554 (ϵ = 7.5), 606 (ϵ = 5.2).

X-ray Structure Determinations. Both X-ray studies were carried out on an ENRAF-Nonius CAD4 diffractometer using graphite monochromatized Mo Kα radiation. The cell parameters were obtained by fitting a set of 25 high-θ reflections. Crystallographic data are collected in Table 1. Crystals of the compounds were obtained as reported in results. Atomic scattering factors were from *International Tables for X-ray Crystallography*. The calculations were performed on a Hewlett Packard 9000-710 for structure determination and on a digital MicroVaX 3100 with the MolEN package[22] for refinement and ORTEP calculations.

Single-Crystal Structure Determination on $[(PPh(OMe)_2)_2Fe(T(p\text{-}Me)PP)]CF_3SO_3$, 1. The data collection ($2\theta_{max}$ = 50°, scan $\omega/2\theta$ = 1, t_{max} = 60 s, range h, k, l: h = −19.19, k = 0.19, l = 0.24, intensity controls without appreciable decay (0.4%) gave 7335 reflections from which 3987 reflections satisfied $I > 3\sigma(I)$. After Lorentz and polarization corrections, the structure was solved with direct methods[23] which reveal the Fe, P, and some C atoms. The remaining nonhydrogen atoms of the structure, the triflate anion, and the two solvent molecules were found after successive scale for factor refinements and Fourier difference. After isotropic (R = 0.095), then anisotropic refinement (R = 0.076), some hydrogen atoms were found with a Fourier difference; the remaining ones were set in geometrical position and not refined. The whole structure was refined by the full-matrix least-square techniques (use of F magnitude; x, y, z, $\beta_{i,j}$ for Fe, P, O, N and C atoms; x, y, z for triflate anion and x, y, z for hydrogen atoms; 741 variables and 3987 observations; $w = 1/\sigma(F_o)^2 = [\sigma^2(I) + (0.04F_o^2)^2]^{-1/2}$) with the resulting R = 0.066, R_w = 0.062, and S_w = 2.72 (residual $\Delta\rho$ < 0.33 e Å^{-3}).

Single-Crystal Structure Determination on $[(PPh(OEt)_2)_2Fe(T(p\text{-}Me)PP)]CF_3SO_3$, 2. The data collection ($2\theta_{max}$ = 54°, scan $\omega/2\theta$ = 1, t_{max} = 60 s, range h, k, l: h = −28.28, k = 0.17, l = 0.22, intensity controls without appreciable decay (12%) gave 10297 reflections from which 4334 reflections satisfied $I > 3\sigma(I)$. After Lorentz and polarization corrections, the structure was solved with direct methods[23] which reveal the Fe, P, and some C atoms. The remaining nonhydrogen atoms of the structure were found after successive scale for factor refinements and Fourier difference. The triflate anion was found as disordered in two positions. After isotropic (R = 0.125), then anisotropic refinement (R = 0.096), some hydrogen atoms were found with a Fourier difference; the remaining ones were set in geometrical position and not refined. The whole structure was refined by the full-matrix least-square techniques (use of F magnitude; x, y, z, $\beta_{i,j}$ for Fe, P, O, N, and C atoms; x, y, z for triflate anion and x, y, z for hydrogen atoms; 769 variables and 4334 observations; $w = 1/\sigma(F_o)^2 = [\sigma^2(I) + (0.04F_o^2)^2]^{-1/2}$) with the resulting R = 0.072, R_w = 0.069, and S_w = 4.53 (residual $\Delta\rho$ < 0.63 e Å^{-3}).

Results

Synthesis. The general synthetic strategy with the phosphonite derivatives reported herein was to choose *meso*-(tetraphenylporphyrinato)iron^{III} ligated by weakly coordinating counterions (perchlorate or triflate) as intermediates, which made possible product isolation. Actually three major difficulties that we have encountered in preparing phosphonite ferric derivatives have been (i) autoreduction to the ferrous state, (ii) the necessity to add a large excess of the ligand to assure full complexation, and (iii) the partial hydrolysis of the phosphonite to the phosphinic ester in the presence of traces of acidic water. In the latter case the product was the perchlorato derivative of bis(phenylphosphinic methyl ester) (tetraphenylporphyrinato)iron^{III}, which is a new high-spin six-coordinate ferric porphyrin.[24] When these problems are controlled, addition under argon of 8 equiv of dimethyl phenylphosphonite to $[Fe(TPP)]ClO_4$ in dichloromethane affords the hexacoordinated complex $[(P(OMe)_2Ph)_2Fe(TPP)]ClO_4$ with 74% yield. For the preparation of the other ferriporphyrin derivatives with this phosphonite, $[(P(OMe)_2Ph)_2Fe(T(m\text{-}Me)PP)]ClO_4$ and $[(P(OMe)_2Ph)_2Fe(T(p\text{-}Me)PP)]ClO_4$, the same procedure can be used. The need for an X-ray crystal structure of at least one derivative led us to extend this reaction to the complexation of a second ligand, diethylphenylphosphonite, and to the use of triflate as anion. Finally, under similar reaction conditions, the complete X-ray structural analyses of two derivatives, $[(PPh(OMe)_2)_2Fe(T(p\text{-}Me)PP)]CF_3SO_3$, **1**, and $[(PPh(OEt)_2)_2Fe(T(p\text{-}Me)PP)]CF_3SO_3$, **2**, were successful. The triflate anion was used for reason of safety, although most of the physical measurements have been performed on the low-spin ferric porphyrin family with perchlorate anions.[9]

Stuctures of the Bis(phosphonite) Complexes. The molecular structures of $[(PPh(OMe)_2)_2Fe(T(p\text{-}Me)PP)]CF_3SO_3$, **1**, and $[(PPh(OEt)_2)_2Fe(T(p\text{-}Me)PP)]CF_3SO_3$, **2**, are shown in the ORTEP diagram (Figures 1 and 2) along with the numbering scheme for the crystallographically unique atoms. As can be

(22) *ENRAF-NONIUS Molecular Determination Package*; Delft University, The Netherlands (current version: 1990).

(23) Sheldrick, G. M. In *Crystallographic Computing 3: Data Collection, Structure Determination, Proteins and Databases*; Sheldrick, G. M., Krüger, C., Goddard, R., Eds; Clarendon Press: Oxford, 1985.

(24) Guillemot, M.; Toupet, L.; Simonneaux, G. *Inorg. Chem.* **1996**, *35*, 6334.

Table 2. Selected Bond Lengths and Distances in $[(P(OMe)_2Ph)_2Fe(T(p\text{-}Me)PP)]CF_3SO_3$, **1**, and $[(P(OEt)_2Ph)_2Fe(T(p\text{-}Me)PP)]CF_3SO_3$, **2a**

Distances, Å

bond	**1**	**2**	bond	**1**	**2**
Fe−N(1)	1.967(6)	1.988(6)	Fe−N(4)	1.982(7)	1.971(7)
Fe−N(2)	1.962(2)	1.966(7)	Fe−P(1)	2.293(3)	2.329(3)
Fe−N(3)	1.976(6)	1.954(6)	Fe−P(2)	2.313(4)	2.326(3)

Angles, deg

angle	**1**	**2**	angle	**1**	**2**
N(1)−Fe−N(2)	89.9(3)	89.7(3)	P(1)−Fe−N(3)	88.1(3)	92.6(2)
N(1)−Fe−N(3)	178.6(4)	179.0(3)	P(1)−Fe−N(4)	86.5(3)	90.7(2)
N(1)−Fe−N(4)	90.4(3)	90.0(3)	P(2)−Fe−N(1)	91.0(3)	87.0(2)
N(2)−Fe−N(3)	90.3(3)	89.9(3)	P(2)−Fe−N(2)	88.2(3)	91.3(2)
N(2)−Fe−N(4)	179.5(3)	179.3(3)	P(2)−Fe−N(3)	87.6(3)	92.1(2)
N(3)−Fe−N(4)	89.4(3)	90.4(3)	P(2)−Fe−N(4)	92.2(3)	89.3(2)
P(1)−Fe−N(1)	93.3(3)	88.3(2)	P(1)−Fe−P(2)	175.49(8)	175.3(1)
P(1)−Fe−N(2)	93.1(3)	88.7(2)			

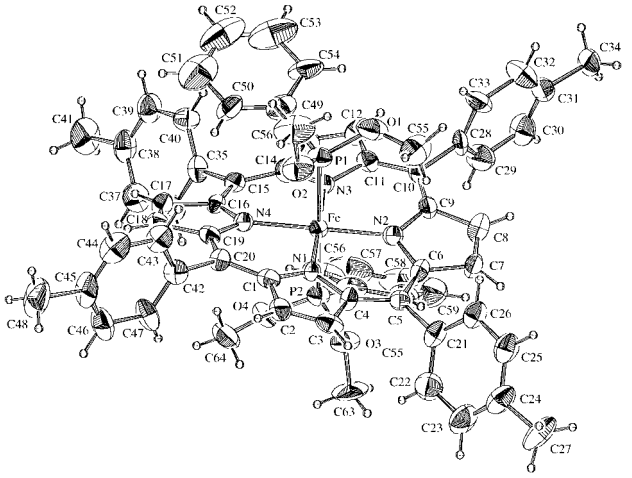

Figure 1. ORTEP diagram of $[(PPh(OMe)_2)_2Fe(T(p\text{-}Me)PP)]CF_3SO_3$, **1**. Labels assigned to the crystallographically unique atoms are displayed. Atoms are contoured at the 50% probability level.

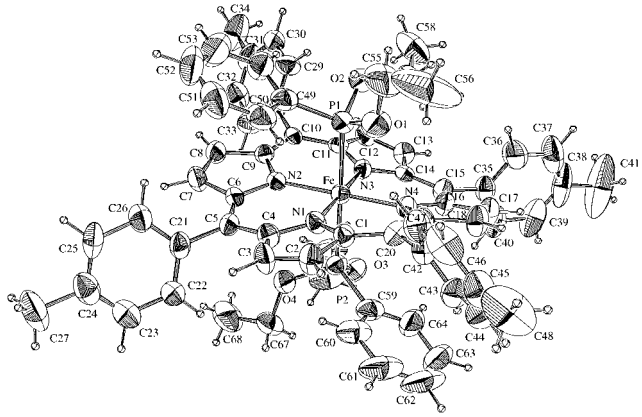

Figure 2. ORTEP diagram of $[(PPh(OEt)_2)_2Fe(T(p\text{-}Me)PP)]CF_3SO_3$, **2**. Labels assigned to the crystallographically unique atoms are displayed. Atoms are contoured at the 50% probability level.

seen in Figures 1 and 2, the molecular structures of the two compounds, including all significant conformational aspects, are quite similar. The phenyl ring of the axial ligand is oriented so that it minimizes the steric interaction with two adjacent porphyrinate phenyl rings. The dihedral angles between the porphyrinate plane and the plane of the four phenyl rings are 88.5(3), 111.7(3), 63.7(3), and 99.2(3)° for **1** and 109.2(3), 66.3(2), 85.8(3), and 118.3(3) ° for **2**; these are well removed from 90°, but these values are not unusual.

Individual values of bond distances and angles for $[(PPh(OMe)_2)_2Fe(T(p\text{-}Me)PP)]\ CF_3SO_3$, **1**, and for $[(PPh(OEt)_2)_2Fe(T(p\text{-}Me)PP)]CF_3SO_3$, **2**, are given in Table 2. The metal−phosphorus bond length [2.303 Å] for **1** and [2.326 Å] for **2** are shorter than those observed in the analogous iron^{III} complex containing dimethylphosphine ligand [2.350 Å].[6d] This is consistent with the greater π-acceptor ability of phosphonite ligands compared with that of phosphine ligands and with a concomitant increase in π back-bonding from iron to the axial ligand.

The equatorial Fe−N bond distances average to 1.971(6) Å for **1** and to 1.969(7) Å for **2**, which is quite short for low-spin iron(III) porphyrinate derivatives.[25] These short distances are consistent with the large ruffling of the porphyrinate core, which is very similar to that recently reported in perchlorato derivatives of bis(pyridine)(tetraphenylporphyrinato)iron^{III} [13c] and of bis(isocyanide)(tetraphenylporphyrinato)iron^{III}.[12] Deviation of each unique atom from the mean plane of the core for **1** and **2** is shown in Figure 3, parts a and b, respectively. The ruffling of the core is quite apparent in both complexes and similar to the ruffling observed in $[(4\text{-}CN\text{-}Py)_2Fe(TPP)]\ ClO_4$.[13c] In order to further test the hypothesis that the ruffled core in phosphonite complexes results from an electronic effect, a comparison with a previously determined X-ray structure of $[(PPh(Me)_2)_2Fe(TPP)]ClO_4$[6d] is worthwhile. As is also seen in Figure 3, part c, the ruffling is very weak in this complex. A related ferrous compound $(P(OMe)_3)_2Fe(T(p\text{-}OMe)PP)$, which is diamagnetic, also does not show any ruffling.[26]

^{1}H NMR Spectra of the Bis(phosphonite) Complexes. The ^{1}H NMR spectrum of $[(P(OEt)_2Ph)_2Fe(T(p\text{-}Me)PP)]CF_3SO_3$, **2**, is shown in Figure 4 and the isotropic shifts are listed in Table 3. The peaks for the phenyl protons of the porphyrin ring are assigned unambiguously by methyl substitution and in combination with proton decoupled experiments. For phosphonite axial ligands, measurements of the relative intensities and relative line widths completely determine the assignment. The chemical shift of the phosphonite ligand is totally independent of excess ligand. Hence axial ligand dissociation is not expected to become significant at ambient temperature. The CH_2 groups of the axial ligands appear as two signals at 20°C and as a single broad signal at −60 °C. It should be noted that the ^{1}H NMR spectrum of the free ligand shows also two multiplets for the CH_2 groups that is probably due to diastereoisomerism.

The spectrum of **2** shows unexpected behavior in that the pyrrole proton signal is found in a downfield position at −2 ppm (20 °C). It contrasts with the pyrrole proton of that of $[(P(Me)_2Ph)_2Fe(TPP)]ClO_4$ (δ = −19.4 ppm)[6c] and provides

(25) Scheidt,W. R.; Reed, C. A. *Chem. Rev.* **1981**, *81*, 543.
(26) Toupet, L.; Legrand, N.; Bondon, A.; Simonneaux, G. *Acta Crystallogr.* **1994,** *C50*, 1014.

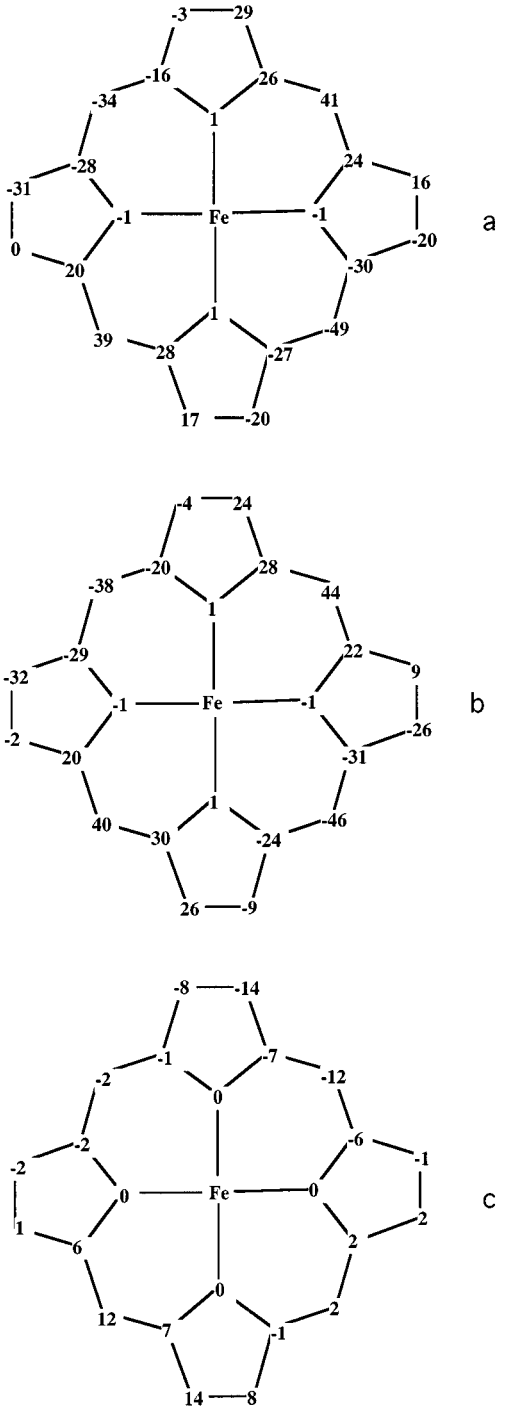

Figure 3. Formal diagram of the porphyrinato core in [(PPh(OMe)$_2$)$_2$Fe(T(*p*-Me)PP)]CF_3SO_3, **1** (part a), [(PPh(OEt)$_2$)$_2$Fe(T(*p*-Me)PP)]CF_3SO_3, **2** (part b), and [(PPh(Me)$_2$)$_2$Fe(TPP)]ClO_4, **3** (part c), showing deviations of each unique atom from the mean plane of the core (units: 0.01).

an essential proof for a different electronic structure in these derivatives. Similar results were obtained with [(P(OMe)$_2$Ph)$_2$Fe(TPP)]ClO_4. In this case, the pyrrole proton signal is found in a more downfield position at + 3 ppm (20 °C).[17] Evans' magnetic measurements[27] were made for 0.03 M CD_2Cl_2 solutions of [(P(OEt)$_2$Ph)$_2$ Fe(TPP)]CF_3SO_3 employing Me_4Si as the reference (20 °C). The solution magnetic moment (μ = 1.90 μ_B) is compatible with the low-spin state $S = {}^1/_2$. Analysis of the curve in the Curie plot was made for the two derivatives [(P(OMe)$_2$Ph)$_2$Fe(TPP)]ClO_4 and [(P(OEt)$_2$Ph)$_2$Fe(T(*p*-Me)PP)]CF_3SO_3, **2**, complexes. The temperature dependences of the isotropic shifts of the protons of **2** in CD_2Cl_2 are shown in Figure 5. The isotropic shifts vary linearly with $1/T$, but the extrapoled lines do not pass through the origin at $1/T = 0$ and the pyrrole protons show an anti-Curie behavior.

In order to characterize the iron bis-phosphonite electronic structure, the isotropic shifts were calculated for **2** by using (P(OMe)$_2$Ph)$_2$ Fe(TPP) and related *para* and *meta*-methyl substituted diamagnetic complexes as references.[24] Analysis of the chemical shift was made according to the method of La Mar.[10] In this method, the plot $(\Delta H/H)_{iso}$ vs $(3\cos^2\theta - 1)/r^3$ for all proton *meso*-aryl positions (and methyl substituents) permits a quantitative separation of the dipolar and contact contributions to the hyperfine shift (supplementary material). The results are summarized in Table 3. It is clearly observed for 2 that there is a relatively large contact contribution to the *meso*-phenyl-H resonances. It is interesting to note that the mechanism of spin transfer appears here to be significantly different from that observed for low-spin ferric bis(phosphine) complexes of synthetic porphyrins.[6c] In this latter case, the phenyl proton shifts of [(PMe_3)$_2$Fe(TPP)]ClO_4 were found to be essentially dipolar in origin, with a weak contact contribution in the para position.[6c] Using the *o*-H dipolar shift and the relative geometric factors,[9] the dipolar contribution to pyrrole-H can be obtained via the relation $(\Delta H/H)^i_{dip} = (\Delta H/H)^{o\text{-}H}_{dip}\,[(3\cos^2\theta - 1)r^{-3}]_i/[(3\cos^2\theta - 1)r^{-3}]_{o\text{-}H}$. The resulting dipolar and contact contributions are also included in Table 3.

UV−Vis Spectroscopy. The [(P(OMe)$_2$Ph)$_2$Fe(TPP)]ClO_4 complex exhibited hyperspectra[28] with two Soret bands, one at 437 nm (ϵ = 5.9 10^4 M^{-1} cm^{-1}) and the second in the near-ultraviolet region (357 nm, ϵ = 2.8 10^4 M^{-1} cm^{-1}). All the other phosphonite derivatives show similar behavior. As previously reported for the ferrous state, the presence of two phosphorus ligands in the ferric state gave an hyperspectrum.[6c] Hyper porphyrin spectra for bismercaptide and mercaptide phosphine hemin complexes have been also reported.[6a,b]

EPR Spectroscopy. The EPR spectra of [(PPh(OMe)$_2$)$_2$Fe(T(*p*-Me)PP)]CF_3SO_3 **1** and [(PPh(OEt)$_2$)$_2$Fe(T(*p*-Me)PP)]CF_3SO_3 **2** in solution are unusual since they are axial, with $g_\perp$ = 2.36 and $g_{||}$ = 1.87 for **1** at 4 K, Σg^2 = 14.67 for **1** and Σg^2 = 14.82 for **2**. The spectrum of complex **2** is shown in Figure 6. The relative energies of the three t_{2g} d orbitals can be calculated from the *g* values in solution, using a general theory first elaborated by Griffith[29a] and Taylor[29b] and recently developed by Walker.[9] Using this theory, Δ/λ is negative (−5.5) indicating that d_{xz} and d_{yz} are lower in energy than d_{xy} and thus that the ground state is largely $(d_{xz},d_{yz})^4(d_{xy})^1$. Table 4 presents the EPR parameters of the two complexes [(PPh(OMe)$_2$)$_2$Fe(T(*p*-Me)PP)]CF_3SO_3, **1**, and [(PPh(OEt)$_2$)$_2$Fe(T(*p*-Me)PP)]CF_3SO_3, **2**.

Mössbauer Spectroscopy. Figure 7 shows the Mössbauer spectra of polycrystalline [(PPh(OMe)$_2$)$_2$Fe(T(*p*-Me)PP)]CF_3SO_3 and [(PPh(OEt)$_2$)$_2$Fe(T(*p*-Me)PP)]CF_3SO_3 at 80 K in zero field. The isomer shift and the quadrupole splitting obtained for the two derivatives at 80 K are given in Table 4. The asymmetry observed at 80 K is typical of species having intermediate relaxation effects.[30−33] There was also a consistent decrease in QS with increasing temperature, which is typical

(27) Evans, D. F. *J. Chem. Soc.* **1959**, 2003.

(28) Gouterman, M. In *The Porphyrins*; Dolphin, D., Ed.; Academic Press: New York, 1979; Vol. III, Part A, 1−156.

(29) (a) Griffith, J. S. *Proc. R. Soc. London, Ser. A* **1956**, *235*, 23. (b) Taylor, C. P. S. *Biochim. Biophys. Acta* **1977**, *91*, 165.

(30) Epstein, L. M.; Straub, D. K. *Inorg. Chem.* **1967**, *6*, 1720.

(31) (a) Sams, J. R.; Tsin, T. B. Mössbauer Spectroscopy of Iron Porphyrins. In *The Porphyrins*; Dolphin, D., Ed.; Academic Press: New York, 1978; Vol. IV, pp 425−478. (b) Debrunner, P. G. In *Iron Porphyrins*; Lever, A. B. P., Gray, H. B., Eds.; Physical Bioinorganic Chemistry Series; VCH Publishers: New York, 1989; Part 3, p 137.

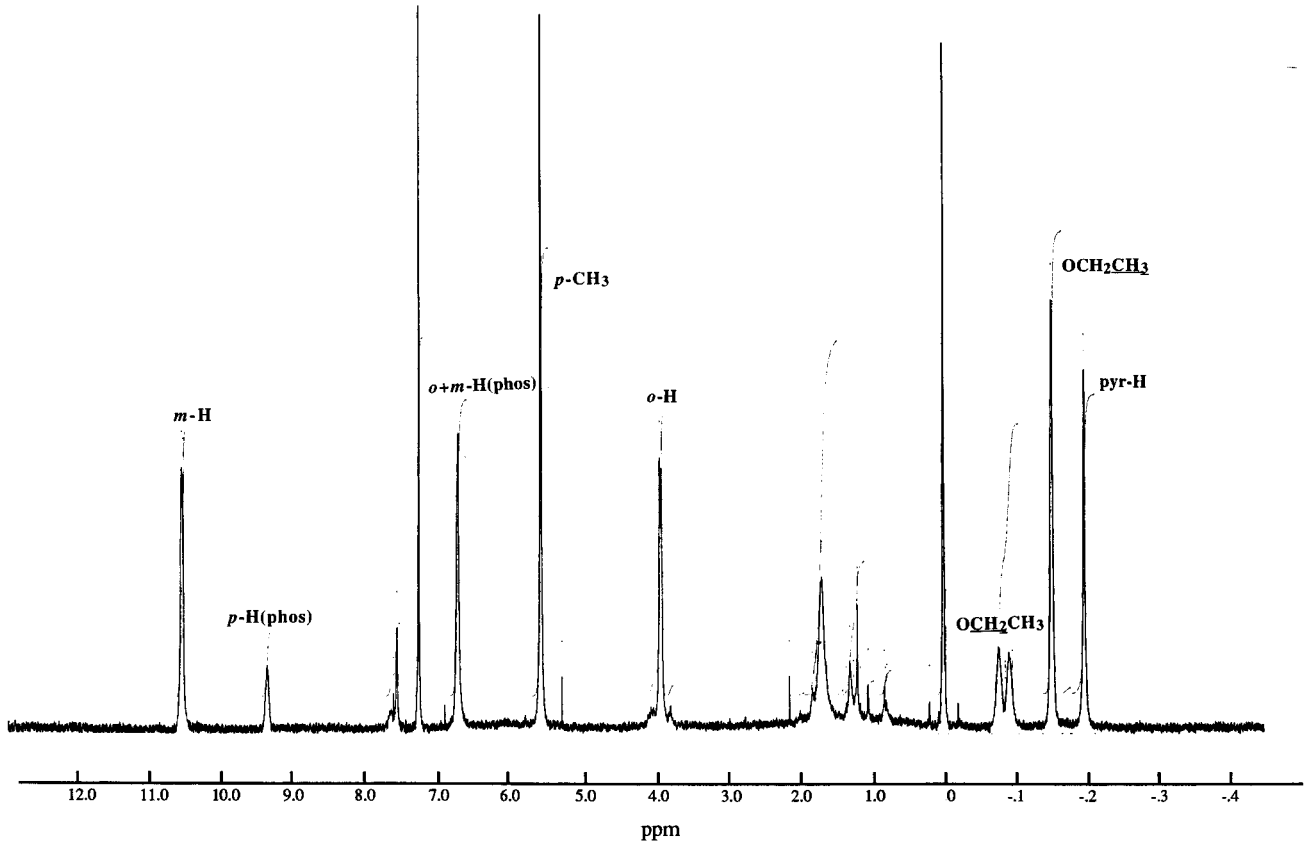

Figure 4. ^{1}H NMR spectrum of $[(PPh(OEt)_2)_2Fe(T(p\text{-}Me)PP)]CF_3SO_3$, **2**, recorded at 283 K in $CHCl_3$.

Table 3. Observed Shifts and Separation of the Isotropic Shift into Contact and Dipolar Contributions in $[(P(OEt)_2Ph)_2Fe(T(p\text{-}Me)PP)]CF_3SO_3$ in CD_2Cl_2 at 293 K

proton type	$\Delta H/H$[a]	$(\Delta H/H)_{iso}$[b]	$(\Delta H/H)_{dip}$[c]	$(\Delta H/H)_{con}$
o-H	4.07	−3.01	2.32	−5.33
m-H	10.41	2.61	0.99	1.62
	(1.98)[d]	(−0.62)	(0.71)	(−1.33)
p-CH_3	5.49	2.99	0.69	2.30
	(5.77)[e]	(−1.73)	(0.89)	(−2.62)
pyrr-H	−2.01[f]	−10.21	4.53	−14.74

[a] Chemical shifts in ppm at 25 °C. [b] Isotropic shift with the diamagnetic $(PPh(OMe)_2)_2Fe(TPP)$ complex as reference. [c] Based on relative geometric factors $(3\cos^2\theta - 1)/r^3$. [d] *m*-CH_3 shift in parentheses. [e] *p*-H shift in parentheses. [f] Using the *o*-H dipolar shift and the relative geometric factor.

for the sensitive low-spin Fe(III) complexes.[31] The quadrupole splitting of **1** is smaller than the typical values for low-spin ferric hemes.[31]

Discussion

It has long been recognized that varying the substituents on phosphorus ligands can cause marked changes in the behavior of coordination complexes. Both steric and electronic effects need to be considered. However, steric effects can be minimized when unencumbered porphyrins like tetraphenylporphyrins are used. For example, triphenylphosphine complexes of iron(II) and ruthenium(II) porphyrins have been reported.[7e,34] Thus, in the case where electronic effects are dominating, both σ donating and π acidity must be considered. The dependence of the

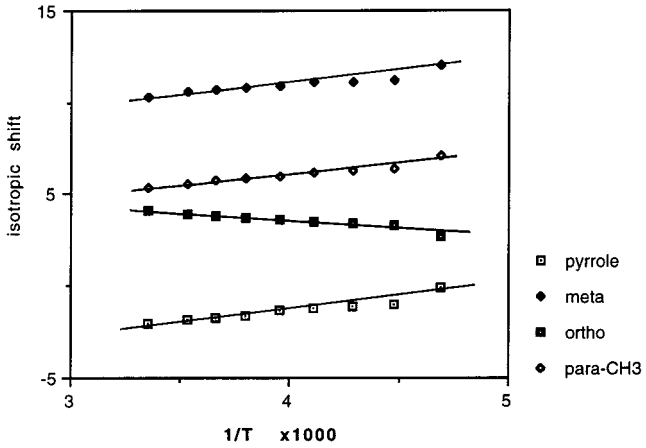

Figure 5. Curie plot of the isotropic shifts vs reciprocal temperature of $[(PPh(OEt)_2)_2Fe(T(p\text{-}Me)PP)]CF_3SO_3$, **2**, in $CHCl_3$.

electronic effect of various PR_3 ligands on the nature of the R group has been quantified by Tolman.[15] For alkyl phosphines, the three donor groups increase the electron density on the metal and the π acidity of the ligand is weak. Unlike PMe_3, phosphites, which have alkoxy groups, are very effective in promoting π acidity.[16] Phosphonites should present an intermediate behavior between trialkyl phosphines and trialkyl phosphites, though only few data are currently available for the latter.[35] The pK_a's of the conjugate acid of the phosphorus ligands decrease in the order $PMe_3 > PMe_2Ph > P(OMe)_2Ph > P(OMe)_3$.[36] The possible electronic interactions of phosphorus ligands with low-spin iron^{III} are the σ donation from the phosphorus lone pair to the empty d_z^2 orbital of iron and back-donation from the filled d_π orbitals of low-spin iron^{III} to the empty d_π orbitals of the phosphorus ligand.[16] Thus $P(OMe)_2$-

(32) Münck, E. Mössbauer Spectra of Hemoproteins. In *The Porphyrins*; Dolphin, D., Ed.; Academic Press: New York, 1978; Vol. IV, pp 379−423.
(33) Maeda, Y. *J. Phys.* **1979,** *40*, 514.
(34) Domatezis, G.; Tarpey, D.; Dolphin, D.; James, B. R. *J. Chem. Soc., Chem. Commun.* **1980**, 939.
(35) Frank, A. W. *Chem. Rev.* **1961**, *61*, 389.

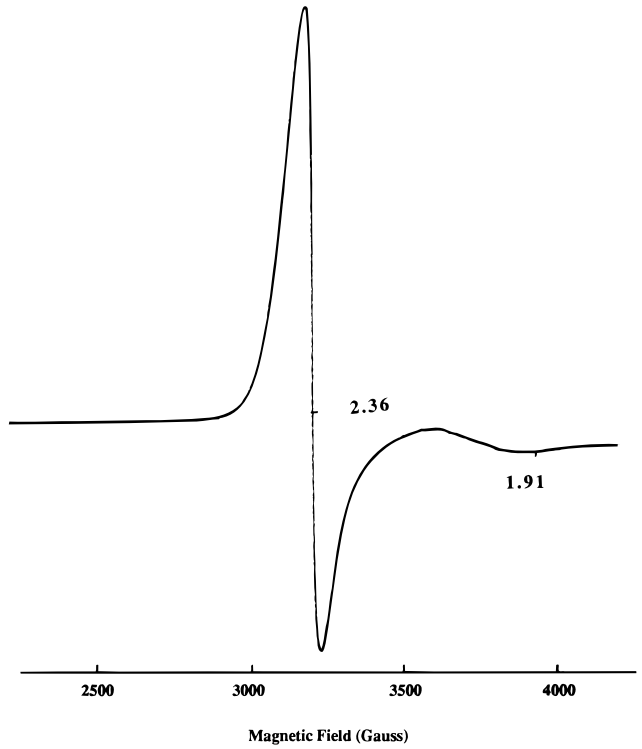

Figure 6. EPR spectrum of $[(PPh(OEt)_2)_2Fe(T(p\text{-}Me)PP)]CF_3SO_3$, **2**, in a CH_2Cl_2 glass, recorded at 4 K.

Table 4. Mössbauer (Polycrystalline) and EPR Data for $[(PPh(OMe)_2)_2Fe(T(p\text{-}Me)PP)]CF_3SO_3$, **1**, and $[(PPh(OEt)_2)_2Fe(T(p\text{-}Me)PP)]CF_3SO_3$, **2**

	1	**2**	
	Mössbauer Data		
T (K)	80	80	4.5
ΔE_Q (mm/s)	1.23	1.66	2.01
δ (mm/s)	0.35	0.37	0.40
	EPR Data (4 K)[a]		
g	2.365	2.365	
g	1.874	1.911	
Σg^2	14.67	14.82	
Δ/λ[b]	−5.1	−5.6	
$\%d_{xy}$	97.8	99.2	

[a] Calculated assuming Taylor's proper axis system, with $g_y = -g_x = g_\perp$ and $g_z = -g_{||}$.[29] [b] Experimental conditions: CH_2Cl_2, 1 mW microwave power; 1.25 mT modulation amplitude.

Ph and $P(OEt)_2Ph$ are expected to be relatively strong π acceptors, while PMe_2Ph is expected to be mainly a σ donor and a moderate π acceptor.

The ruffling observed in the structures of the two compounds **1** and **2** confirms this hypothesis. Strong π acceptor ligands are believed to stabilize the d_{xz} and d_{yz} orbitals to the extent that this energy decrease gives a situation where both orbitals are filled and the d_{xy} orbital has a single vacancy. As a consequence the strong porphyrin $\rightarrow d_{xy}$ π bonding in compounds **1** and **2** leads to a shortening of the ferric ion distance to the pyrrole nitrogen atoms. Such a situation, which was first nicely recognized with the low-spin perchlorato derivative of bis(4-cyanopyridine)(tetraphenylporphyrinato)iron^{III},[13] is accommodated by a ruffling of the porphyrin,[37,38] as evidenced in Figure 3, parts a and b. As expected from the π acidity, the ruffling is even more important for **1** than for **2**. On the other side, ligation of two PMe_2Ph ligands, which are more basic, to the ferric porphyrin yields the compound $[(P(Me)_2Ph)_2Fe(TPP)]ClO_4$ with longer iron−nitrogen bonds 1.990(2) Å (for 1, Fe−N = 1.971 Å and for 2 Fe−N = 1.969 Å) and much less ruffling (Figure 3, part a). Absence of ruffling was also observed in the ferrous bis(phosphite) complex $(P(OMe)_3)_2Fe(TPP)$.[26]

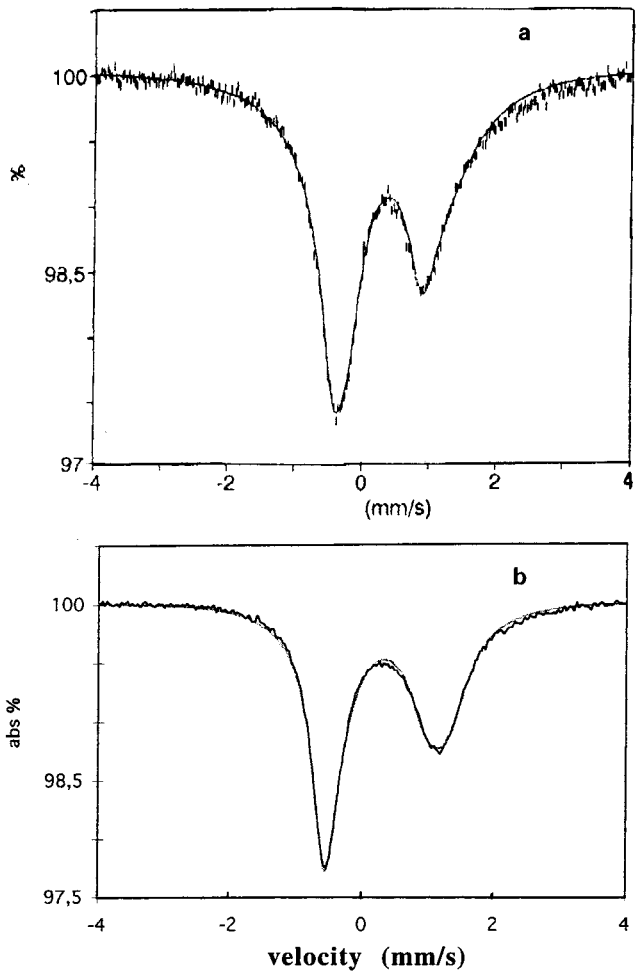

Figure 7. Mössbauer spectra of (a) $[(PPh(OMe)_2)_2Fe(T(p\text{-}Me)PP)]CF_3SO_3$, **1** (part a), and $[(PPh(OEt)_2)_2Fe(T(p\text{-}Me)PP)]CF_3SO_3$, **2** (part b), both recorded at 80 K in zero field.

A similar analysis may describe the ^1H NMR properties of compounds **1** and **2.** The relatively small contact shift for pyrrole protons $\Delta\delta = -6$ ppm for **1** and $\Delta\delta = -5.4$ ppm for **2** ($\Delta\delta = -23$ ppm for $[(PMe_3)_2Fe(TPP)]ClO_4$[6c]) favors the interpretation that only weak spin density is placed on pyrrole carbons and accounts for the observed downfield shift. However the large contact shifts in *meso* phenyl positions which are evident from the data (Table 3), indicate that a large amount of π spin density is placed on the phenyl carbons. This is in contrast with previous work on low-spin ferric derivatives as bis(imidazole) complexes[39] and ferric bis(phosphine) complexes,[6c] for example. As previously reported by us[11] and by Walker and Simonis,[9] this pattern of observed isotropic shifts[40] and the anti-Curie behavior[41] of the pyrrole protons are indicative of a $(d_{xz},d_{yz})^4(d_{xy})^1$ ground state. Different reasons have been suggested to explain this large spin delocalization on the *meso* position, such as an increasing π delocalization on the *meso* carbon positions[10a] or a partial delocalization of the unpaired electron into the (d_{xz},d_{yz}) orbitals.[9] However, a possible contribution of a partial porphyrin π cation radical character to

(36) Rahman, M. M.; Liu, H. Y.; Ericks, K.; Prock, A.; Giering, W. P. *Organometallics* **1989**, *8*, 1.
(37) Collins, D. M.; Scheidt, W. R.; Hoard, J. L. *J. Am. Chem. Soc.* **1972**, *94*, 6689.
(38) Hoard, J. L. *Ann. N.Y. Acad. Sci.* **1973**, *206*, 18.
(39) La Mar, G.; Walker, F. A. *J. Am. Chem. Soc.* **1973**, *95*, 1782.

the electronic configurations of these derivatives has been the current opinion,[13b] although, to our knowledge, the typical visible spectrum of such radical cation has never been observed with these complexes. In order to explain the anti-Curie behavior, the presence of excited states has been recently proposed in several model heme systems having unsymmetrical substitution patterns.[40] The same two level approach could also be applied to our system but the theoretical treatment is beyond this current work. An upfield chemical shift is obtained for the methoxy groups of ligated $P(OMe)_2Ph$. As previously reported for $[(PMe_3)_2Fe(TPP)]ClO_4$,[6c] this may be due to unpaired spin density on the methyl group occurring from the d orbitals, implying that the contact shift is the dominating effect.

It has been recognized that the EPR *g* values of low-spin ferriporphyrins provide valuable information on the nature of the orbital of the unpaired electron.[1,30−34,42] The EPR spectra for complexes **1** and **2** are axial with *g* values very close to each other and very close to 2.0. This is quite different from the classical situation of low-spin ferric porphyrins which have been studied in depth. Usually the electronic configuration of the iron in such low-spin derivatives among the t_{2g} orbitals is $(d_{xy})^2(d_{xz},d_{yz})^3$, which exists as a rhombically distorted system with tetragonal and rhombic splitting parameters.[30−34,42−44] In the complexes with low-basicity phosphonites, we suggested, as previously reported with cyanopyridines and isocyanides,[13c] that the d_{xy} orbital is higher in energy than the d_{xz},d_{yz} pair. This electronic state leads to the novel $(d_{xz},d_{yz})^4(d_{xy})^1$ state where the d_{xz},d_{yz} pair is degenerate. However, a thorough EPR study with a complete series of phosphorus derivatives, going from trialkylphosphines, which are strongly basic, to phosphites and fluorophosphines, which are strong π acceptors, is necessary to relate the amount of π acceptor ability with the localization of the spin density in the t_{2g} orbitals of the metal.

Most Mössbauer studies of low-spin ferric porphyrins give room temperature isomer shifts of about 0.15 mm/s, increasing to about 0.24 mm/s at 77 K.[31] In contrast, complexes **1** and **2** show similar isomer shifts: 0.35 and 0.37 mm/s, respectively, which are clearly higher values. There are, moreover, a few other points that should also be noted. First, the spectra of **1** at 4 K (not shown) and 70 K show unsymmetrical doublets, the left line being broader than the right at 4 K but in the reverse situation at 80 K. Second, the quadrupole splittings, which are generally in the range $QS = 2 \pm 0.3$ mm/s[31] for most of the low-spin ferric derivatives, are smaller for **1** and **2** (Table 4). This may be related to previous work on $[(4\text{-CN-Py})_2Fe(TPP)]ClO_4$.[13b] In this case the low value (0.65 mm/s, 120 K) was indicative of a partial quenching of orbital angular momentum in the ground-state electron configuration of this complex, as is expected for a high percentage of $(d_{xz},d_{yz})^4(d_{xy})^1$. However, any attempt to relate these differences to specific structural features of the phosphonite ligation to ferric porphyrins would require more extensive studies on other phosphorus derivatives, including Mösssbauer under applied magnetic fields.

Conclusion

The unusual properties of the iron^{III} tetraphenylporphyrinates, with isocyanide[11] as axial ligand together with recent results with low-basicity pyridines,[9c] have led us to study the low-basicity phosphonite complexation with iron^{III} tetraphenylporphyrinate derivatives. Unlike phosphines,[6c,d] the π acceptor properties of phosphonites dominate the bonding in low-spin ferric porphyrins leading to the unusual $(d_{xz},d_{yz})^4(d_{xy})^1$ ground state. The X-ray crystal structures and the ^1H NMR and EPR spectra of the two complexes **1** and **2** are consistent with this situation and provide another example of the electronic contribution to the ruffling of a metalloporphyrin.

Acknowledgment. We are grateful to Prof. Ann Walker for useful discussion and Alain Mari (CNRS, Toulouse) for the Mössbauer measurements.

Supporting Information Available: Tables of parameters, positional and thermal parameters for all atoms, anisotropic displacement parameters for non-hydrogen atoms, bond distances and bond angles, and plots of isotropic shifts versus the geometric factors (48 pages). Ordering information is given on any current masthead page.

IC9704849

(40) A recent work on the binding of 2-methylimidazole to *meso*-tetra(alkylporphyrinato)iron chloride also shows pyrrole signals at low-field position and this effect was explained in terms of the nonplanarity of the porphyrin ring: Nakamura, M.; Ikeue, T.; Neha, S.; Funasaki, N.; Nakamura, N. *Inorg. Chem.* **1996**, *35*, 3731.
(41) Shokhirev, N. V.; Walker, F. A. *J. Phys. Chem.* **1995**, *99*, 17795.
(42) (a) Palmer, G. In *The Porphyrins*; Dolphin, D., Ed.; Academic Press: New York, 1979; Vol. IV, pp 313−353. (b) Palmer, G. Electron Paramagnetic Resonance of Hemoproteins. In *Iron Porphyrins*; Lever, A. B. P., Gray, H. B., Eds.; Physical Bioinorganic Series; Addison-Wesley Publishing Company: Reading, MA, 1983; Part 1, pp 43−86.
(43) Muhoberac, B. B. *Arch. Biochem. Biophys.* **1984,** *233*, 682.
(44) Bryn, M. P.; Strouse, C. E. *J. Am. Chem. Soc.* **1981**, *103*, 2633.